



This is a repository copy of *From Au-Thiolate Chains to Thioether Sierpiński Triangles: The Versatile Surface Chemistry of 1,3,5-Tris(4-Mercaptophenyl)Benzene on Au(111)*.

White Rose Research Online URL for this paper:
<http://eprints.whiterose.ac.uk/107570/>

Version: Supplemental Material

Article:

Rastgoo-Lahrood, A., Martsinovich, N., Lischka, M. et al. (8 more authors) (2016) From Au-Thiolate Chains to Thioether Sierpiński Triangles: The Versatile Surface Chemistry of 1,3,5-Tris(4-Mercaptophenyl)Benzene on Au(111). ACS Nano, 10 (12). pp. 10901-10911. ISSN 1936-0851

<https://doi.org/10.1021/acsnano.6b05470>

Reuse

Unless indicated otherwise, fulltext items are protected by copyright with all rights reserved. The copyright exception in section 29 of the Copyright, Designs and Patents Act 1988 allows the making of a single copy solely for the purpose of non-commercial research or private study within the limits of fair dealing. The publisher or other rights-holder may allow further reproduction and re-use of this version - refer to the White Rose Research Online record for this item. Where records identify the publisher as the copyright holder, users can verify any specific terms of use on the publisher's website.

Takedown

If you consider content in White Rose Research Online to be in breach of UK law, please notify us by emailing eprints@whiterose.ac.uk including the URL of the record and the reason for the withdrawal request.



eprints@whiterose.ac.uk
<https://eprints.whiterose.ac.uk/>

From Au-Thiolate Chains to Thioether Sierpiński Triangles: The Versatile Surface Chemistry of 1,3,5-Tris(4-Mercaptophenyl)Benzene on Au(111)

Atena Rastgoo-Lahrood,[†] Natalia Martsinovich,[‡] Matthias Lischka,[†] Johanna Eichhorn,[†] Pawel Szabelski,[#] Damian Nieckarz,[↓] Thomas Strunskus,[↓] Kalpataru Das,[§] Michael Schmittel,[§] Wolfgang M. Heckl,[†] and Markus Lackinger^{†}*

[†]Department of Physics, Technische Universität München, James-Franck-Str. 1, 85748 Garching, Germany; Nanosystems Initiative Munich and Center for NanoScience (CeNS), Schellingstr. 4, 80799 Munich, Germany;

Deutsches Museum, Museumsinsel 1, 80538 Munich, Germany;

[‡]Department of Chemistry, University of Sheffield, Sheffield S3 7HF, UK;

[#]Department of Theoretical Chemistry, Maria Curie-Skłodowska University, Pl. M.C. Skłodowskiej 3, 20-031 Lublin, Poland;

[↓]Supramolecular Chemistry Laboratory, University of Warsaw, Biological and Chemical Research Centre, Zwirki i Wigury 101, 02-089 Warsaw, Poland;

[†]Institute for Materials Science – Multicomponent Materials,
Christian-Albrechts-Universität zu Kiel, Kaiserstr. 2, 24143 Kiel, Germany;

[§]Center of Micro- and Nanochemistry and Engineering, Organische Chemie I,
Universität Siegen, Adolf-Reichwein-Str. 2, 57068 Siegen, Germany;

1. Additional STM Data

Owing to their intermediate bond strength, single S-Au-S linkages are still reversible even at room temperature. This gives rise to dynamic behavior and reconfigurations of the metal-organic structures:

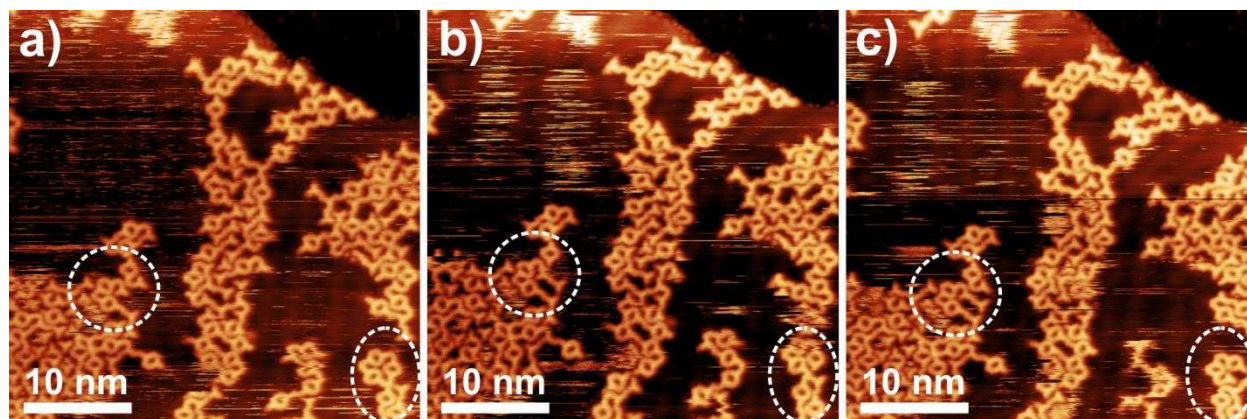


Figure S1. (a) – (c) Series of subsequent STM images of TMB on Au(111) after room temperature deposition acquired from the same sample area (time per frame: ~ 185 s, $V_T = +1.39$ V, $I_T = 47$ pA). The dashed ovals highlight areas with dynamic reconfigurations. In the full series of STM images, growth of a type A chain from top to bottom can be observed in the fuzzy appearing area in the upper left part. A compiled video of the entire series can be downloaded from the Supporting Information.

Sample annealing at 200 °C improved the order and resulted in extended type A and B chains. Type B chains showed a higher tendency for defect formation, whereas type A chains were mostly grouped into molecular braids that were aligned along the herringbone reconstruction.

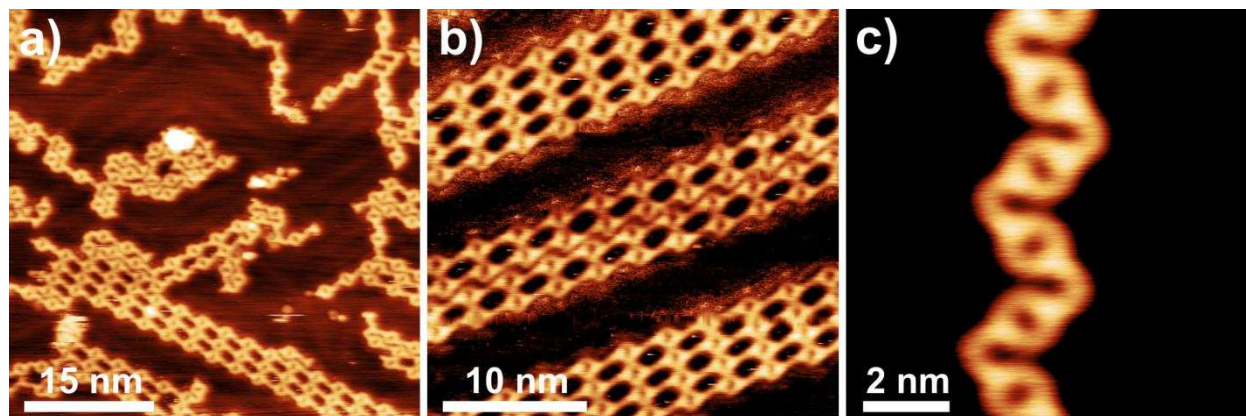


Figure S2. STM images of TMB on Au(111) acquired after annealing at 200 °C. (a) Overview ($V_T = +1.64$ V, $I_T = 38.0$ pA). (b) Close-up of braided type A chains ($V_T = +1.64$ V, $I_T = 37.9$ pA). Interestingly, all four individual type A chains are in phase for the upper and lower braids. (c) Close-up of a defect free segment of a type B chain ($V_T = +1.84$ V, $I_T = 37.6$ pA).

However, annealing at 200 °C not only resulted in extended chains (*cf.* Figure S2 or lower right corner of Figure S3a), but also in less regular aggregates and shorter chain segments. Those appeared either as separate entities or as groups of similarly oriented chains mostly at step-edges (*cf.* Figure S3b). Interestingly these aggregates locally modified the herringbone reconstruction, a further indication for involvement of Au adatoms.

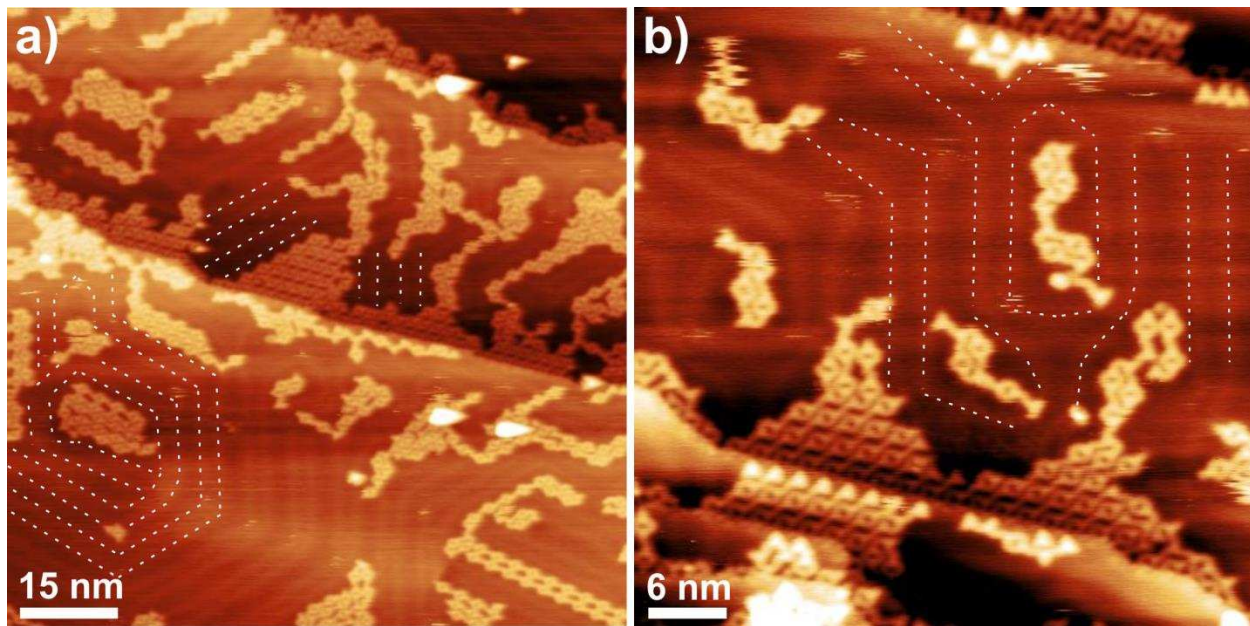


Figure S3. STM images of TMB on Au(111) acquired after annealing at 200 °C. (a) Overview ($V_T = +1.84$ V, $I_T = 37.3$ pA). (b) Close-up ($V_T = +1.67$ V, $I_T = 49.9$ pA). The white dashed lines serve as guides to the eye and mark the soliton lines of the Au(111) herringbone reconstruction.

Further sample annealing at 250 °C resulted in triangular structures on terraces and type C chains aligned along step-edges:

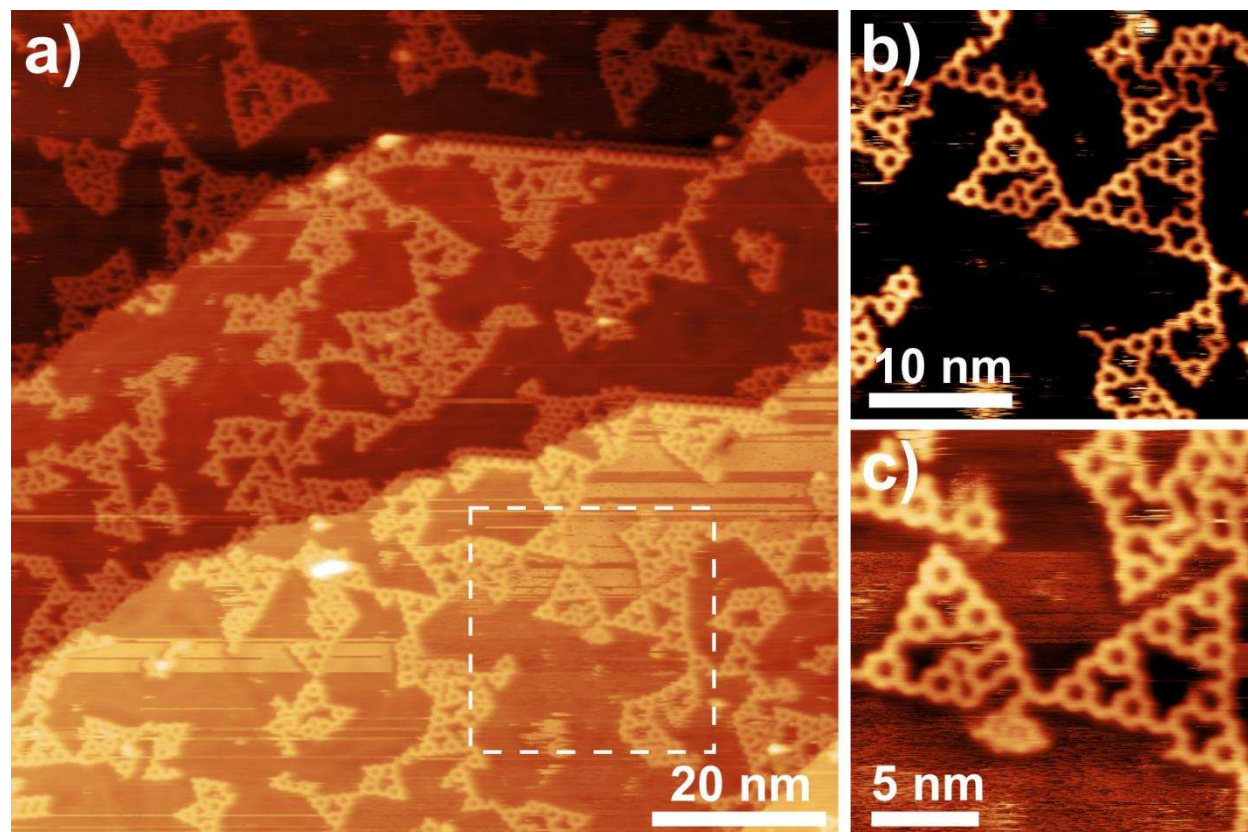


Figure S4. STM images of TMB on Au(111) acquired after annealing at 250 °C. (a) Overview showing the alignment of type C chains along step-edges and STs on terraces ($V_T = +1.47$ V, $I_T = 38.0$ pA). (b) / (c) Close-ups ($V_T = +1.67$ V, $I_T = 37.7$ pA) of the area marked in (a) showing less well defined STs with defects.

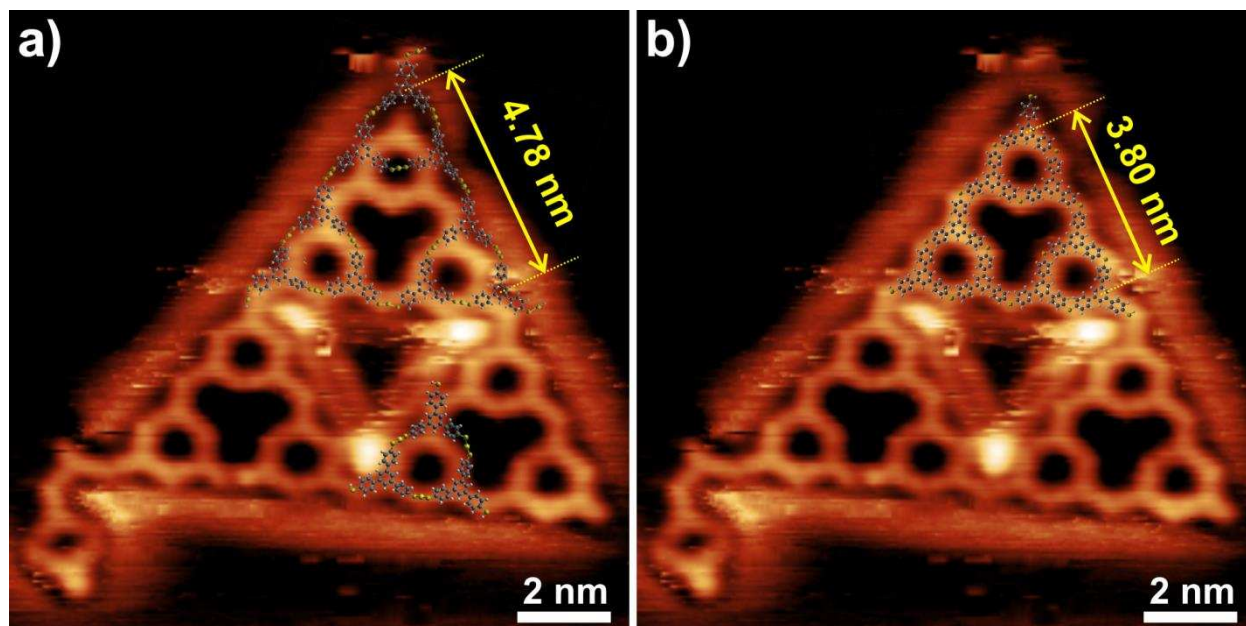


Figure S5. STM image of a second generation ST acquired after room temperature deposition of TMB onto Au(111) and subsequent annealing to 250 °C ($V_T = -1.63$ V, $I_T = 38.1$ pA). The overlays represent DFT optimized geometries. (a) Scaled overlays with models based on coordinative S-Au-S linkages. Both the model of the zero generation ST in the lower half and the model of the first generation ST in the upper half exhibit a center-to-center distance of 1.59 nm between adjacent molecules. As evident from the overlay, these hypothetical metal-organic structures are significantly larger than the experimentally observed structures. (b) Scaled overlay with a model based on covalent C-S-C linkages. The covalent model of the first generation ST features a center-to-center distance of 1.27 nm between adjacent molecules, resulting in a perfect size and geometry match.

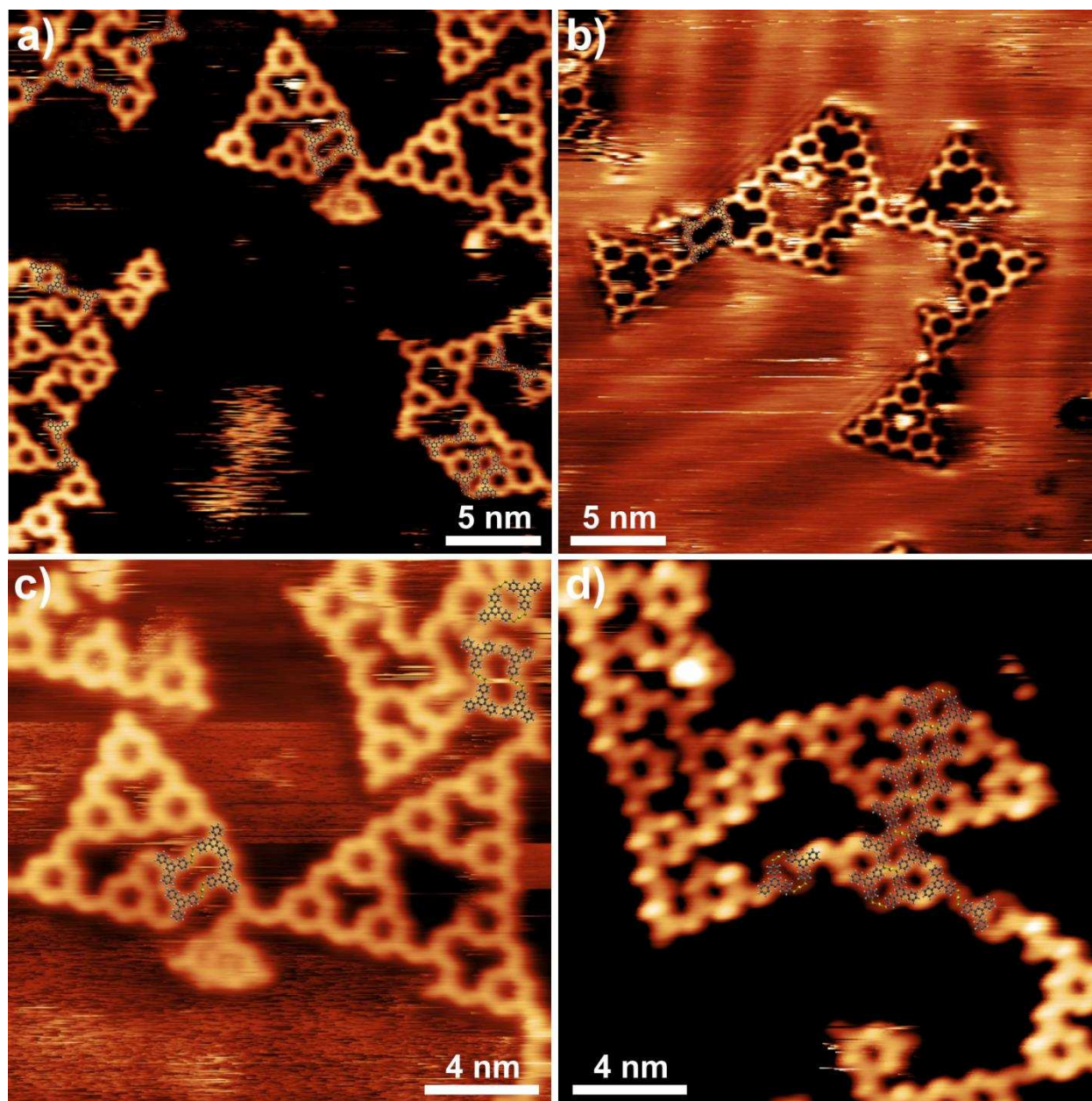


Figure S6. STM images of TMB on Au(111) acquired after annealing at 250 °C. These images demonstrate the coexistence of coordinative S-Au-S and covalent C-S-C linkages. For all overlays the metal-organic dimer motifs 1 and 2 were used. Tunneling parameters: (a) $V_T = +1.67$ V, $I_T = 37.7$ pA; (b) $V_T = +1.60$ V, $I_T = 37.6$ pA; (c) $V_T = +1.67$ V, $I_T = 37.8$ pA; (d) $V_T = -1.97$ V, $I_T = 38.1$ pA;

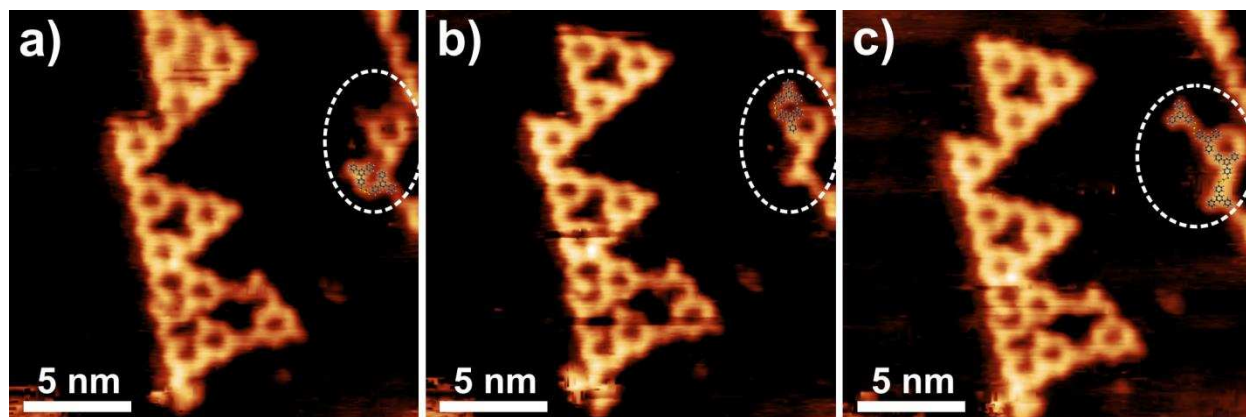


Figure S7. (a) – (c) Series of sequential STM images of TMB on Au(111) acquired after annealing at 250 °C from the same sample area (time between frames: ~204 s, time per frame: ~102 s, $V_T = +1.71$ V, $I_T = 39.8$ pA). The covalent triangular structures on the left hand side do not change between the subsequent images and remain static, whereas the metal-organic structures on the right hand side exhibit dynamic reconfiguration. Provided that all intermediate steps were captured, the following processes were observed: a motif 3 dimer at the lower part decomposes; the released molecule first forms another motif 3 dimer at the upper part that subsequently transforms into a motif 2 dimer.

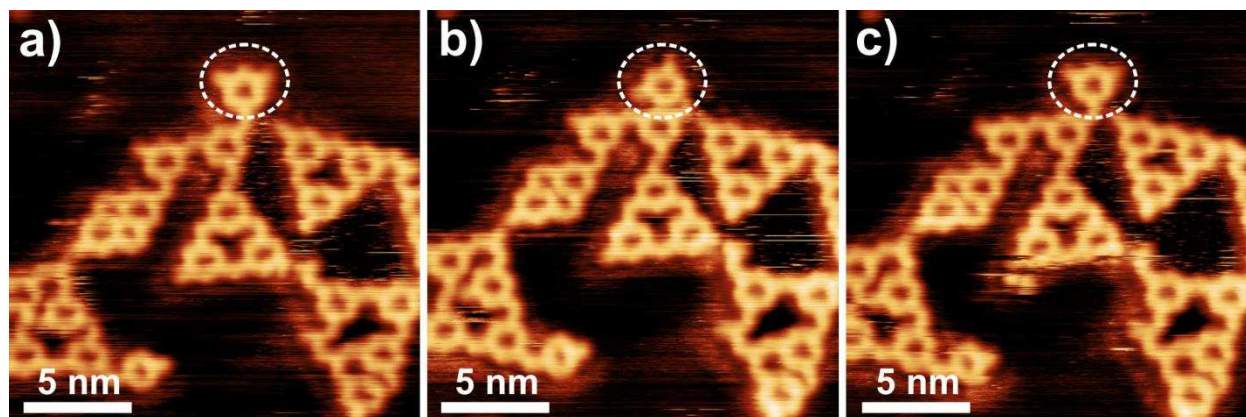


Figure S8. (a) – (c) Series of sequential STM images of TMB on Au(111) acquired after annealing at 250 °C from the same sample area (time in between frames: ~204 s, time per frame: ~102 s; tunneling parameters: (a) $V_T = +1.80$ V, $I_T = 38.7$ pA; (b) $V_T = +1.71$ V, $I_T = 39.7$ pA; (c) $V_T = +1.71$ V, $I_T = 38.7$ pA. This series demonstrates orientational flexibility of a cyclic trimer that is attached to a larger aggregate. The nature of the linkage between trimer and larger aggregate is not entirely clear, but a slightly shorter bond length suggests a covalent C-S-C thioether linkage.

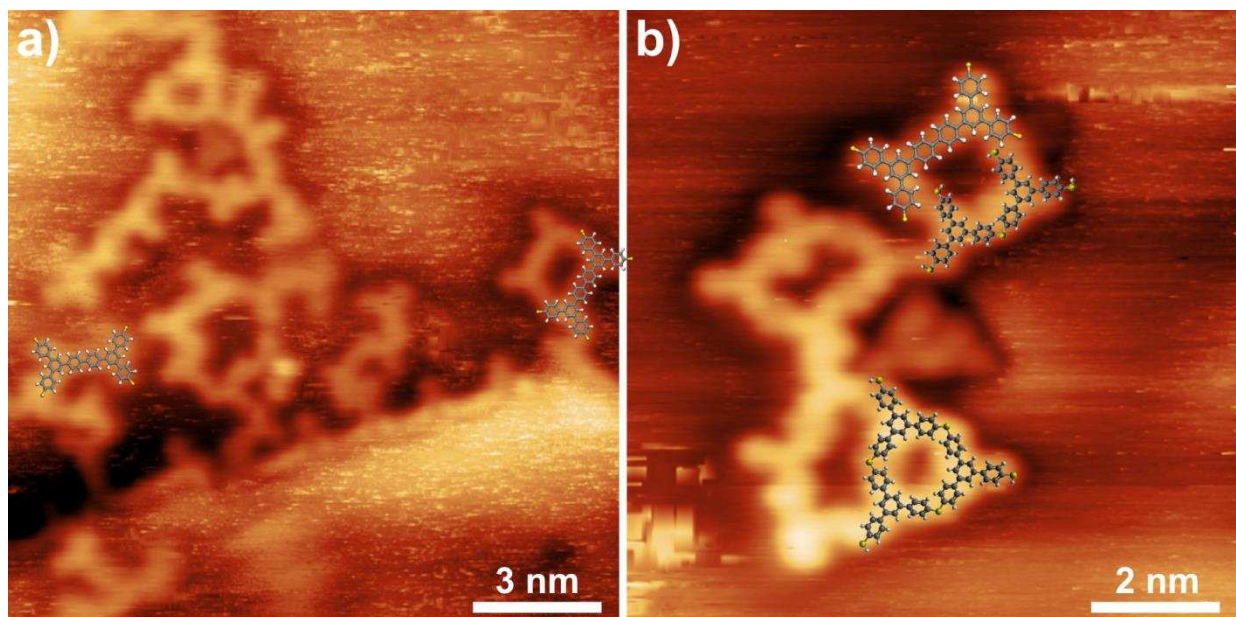


Figure S9. STM images of TMB on Au(111) acquired after annealing at 300 °C from two independent experimental runs. (a) Scaled overlays with covalently C-C linked dimers yield a perfect size and geometry match ($V_T = +1.0$ V, $I_T = 50$ pA). (b) Zoom out of the STM image already shown in the manuscript as Figure 5c ($V_T = +1.63$ V, $I_T = 39.1$ pA). The structure directly underneath the covalently C-C linked dimer matches well with a thioether linked motif 4 dimer. The cyclic trimer at the lower right agrees very well with a covalent zero generation ST based on thioether linkages. The other structures cannot be fitted with these clearly identified motifs, and might thus represent chemically and structurally distinct linkages (*e.g.* disulfur bridges) that cannot unambiguously be identified solely based on STM images.

2. Additional DFT Results

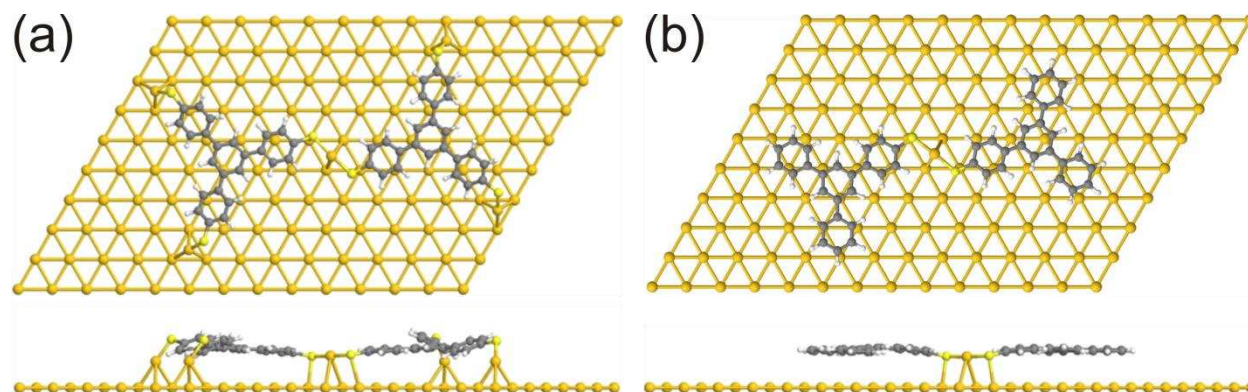


Figure S10. DFT optimized geometries of S-Au-S linked motif 2 dimers on Au(111). The surface was approximated by a single layer of Au(111) with Au atoms frozen in bulk-like positions. Upper and lower rows depict top- and side-views, respectively. Different termini were considered: (a) peripheral thiolate groups that similarly bind to Au adatoms *versus* (b) hydrogen terminated, *i.e.* the peripheral thiolate groups were replaced by hydrogen atoms. Initially, the dimers were placed 0.55 nm above the surface (on average), and adopted the depicted geometries after optimization with the central Au atoms adsorbed in twofold bridge sites. This adsorption geometry also facilitates additional bonds between the sulfur atoms in the S-Au-S linkage and Au surface atoms. Anchoring through the peripheral thiolate groups in (a) imposes additional geometrical constraints, resulting in tilted phenyl rings and a relatively large average carbon adsorption height of 0.351 nm with a similarly large standard deviation of 0.053 nm. In contrast, the hydrogen terminated motif 2 dimer remains almost planar on Au(111) with notably smaller average carbon adsorption height of 0.319 nm and reduced standard deviation of 0.015 nm. The S-Au adatom bond lengths amount to 0.233 nm for (a) and 0.234 nm for (b), respectively.

3. Monte Carlo Simulations

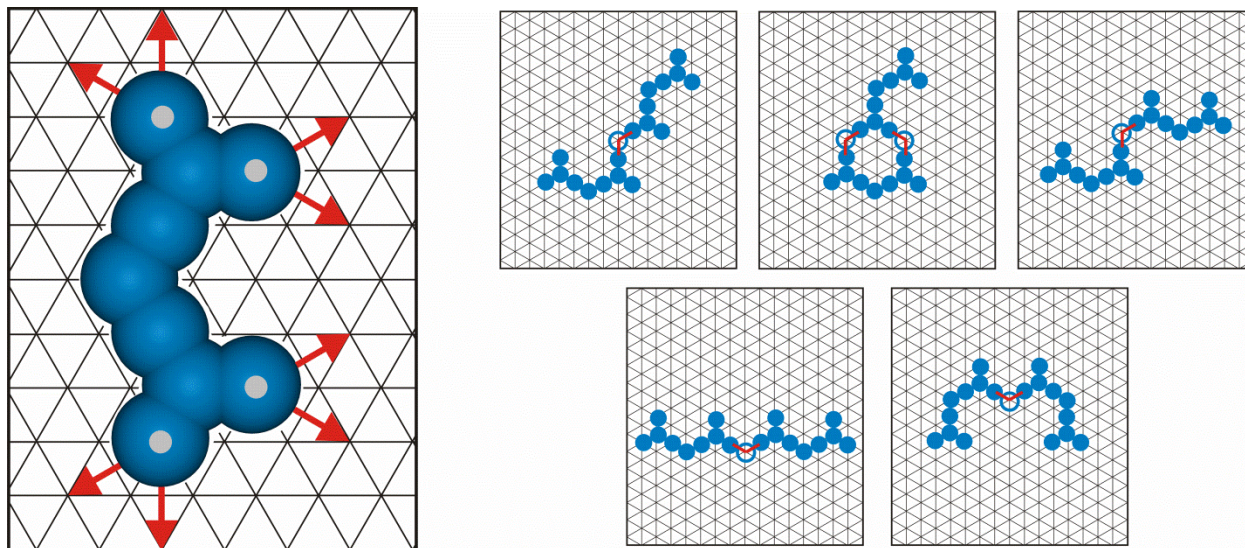


Figure S11. (left) Schematic representation of the thioether linked dimer used as basic building block in MC simulations. Dimers consist of nine interconnected segments that represent the eight phenyl rings and the sulfur atom of the internal thioether linkage, respectively. Dimers can form intermolecular bonds at their four terminal segments (marked with grey dots) in the directions indicated by the red arrows. The right hand side depicts examples for allowed bond configurations between dimers featuring an overall bond angle of 120° (indicated by the red lines). Note that the sulfur atoms of the inter-dimer thioether linkages are not explicitly taken into account. However, all allowed bond configurations feature an empty lattice site at the position of the linking sulfur atom (marked by blue circles) that can be viewed as virtual sulfur atoms.

The following comparisons illustrate similarities between MC simulations and experimental STM images.

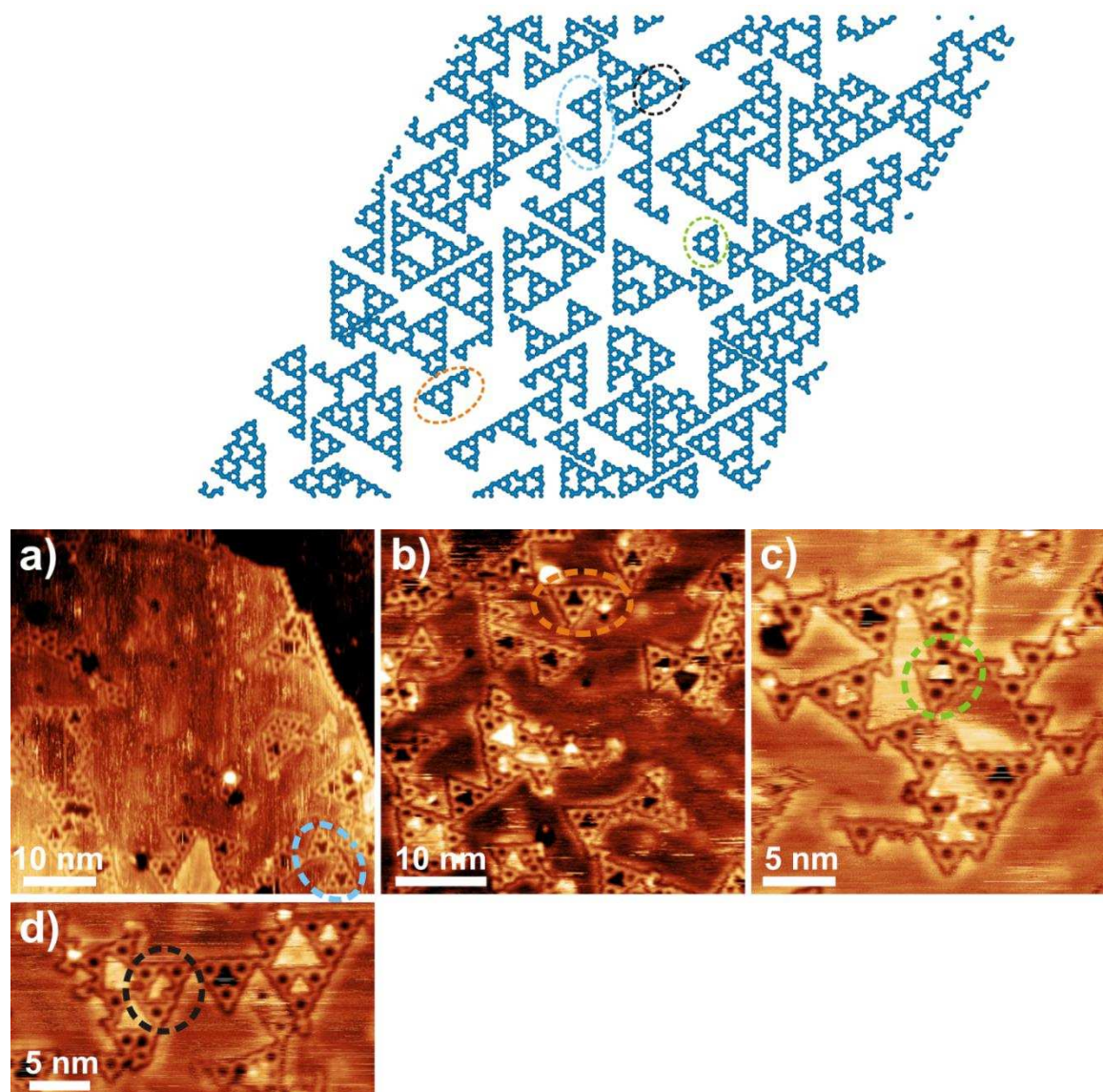


Figure S12. Upper part: MC simulation based on dimers as basic building blocks. The sulfur atoms in the thioether linkages are not depicted for clarity. Lower part: STM images of TMB on Au(111) acquired after annealing at 230°C. Tunneling parameters: (a) $V_T = +1.00$ V, $I_T = 40$ pA; (b) – (d) $V_T = +1.00$ V, $I_T = 50$ pA; The dashed ovals mark aggregates that were similarly observed in both experiment and simulation.

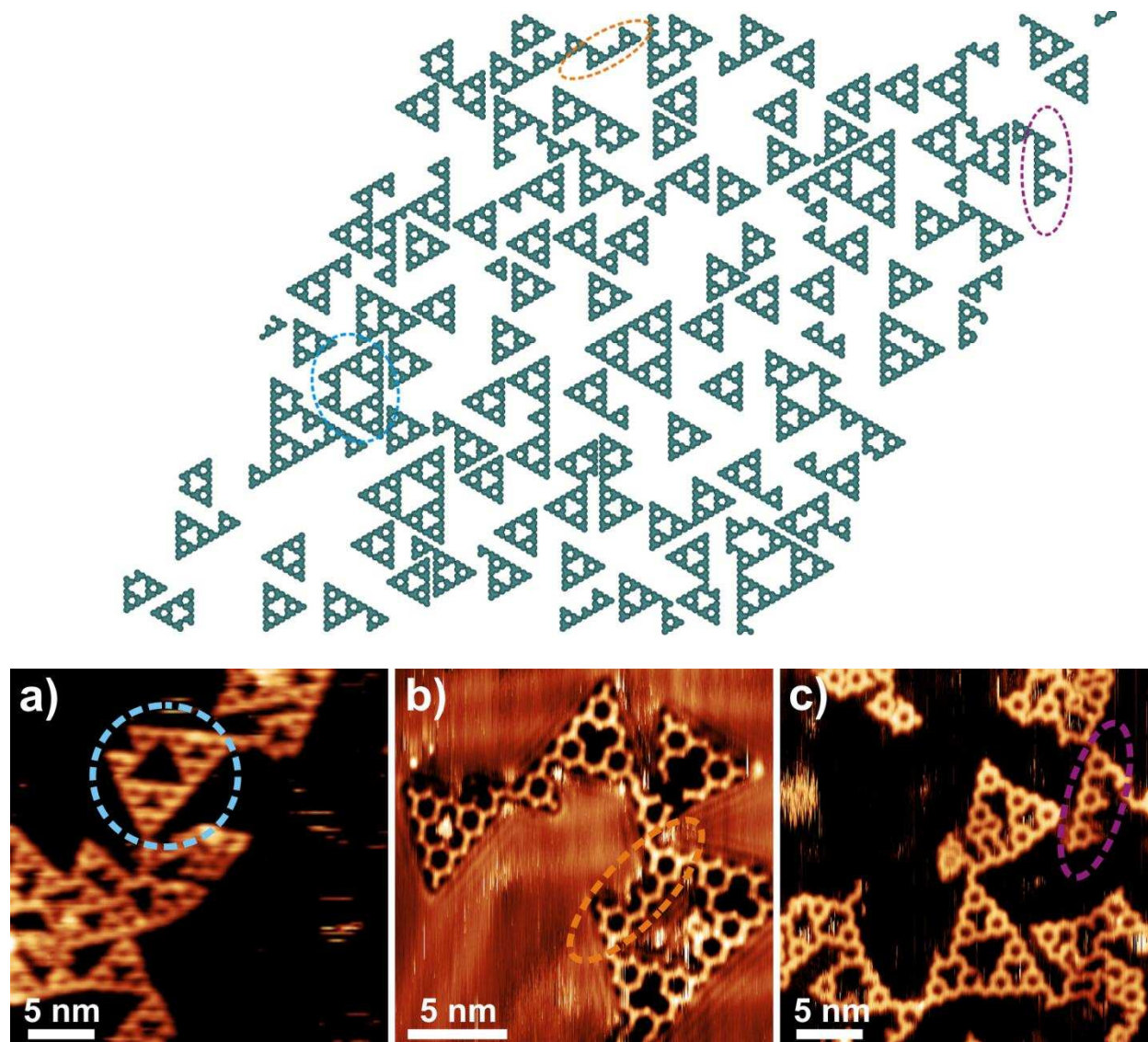


Figure S13. Upper part: MC simulation based on monomers as basic building blocks. The sulfur atoms in the thioether linkages are not depicted for clarity. Lower part: STM images of TMB on Au(111) acquired after annealing at 250°C. The MC simulations with monomers and dimers are essentially similar. However, for the monomer simulation the growing aggregates were not allowed to move or rotate anymore already from the dimer stage on. Tunneling parameters: (a) $V_T = +1.69$ V, $I_T = 37.5$ pA; (b) $V_T = +1.6$ V, $I_T = 37.9$ pA; (c) $V_T = +1.67$ V, $I_T = 37.7$ pA; The dashed ovals mark aggregates that were similarly observed in both experiment and simulation.